1

The Dynamics of the Quiet Solar Chromosphere

W. Kalkofen, Harvard-Smithsonian CfA, S. S. Hasan, Indian Institute of Astrophysics & P. Ulmschneider, Heidelberg
date: 20 December 2001

Abstract: The chapter discusses waves and oscillations in the nonmagnetic (internetwork) chromosphere and in the magnetic network. In the internetwork medium, the waves are acoustic; and in the magnetic network, which is idealized in terms of thin magnetic flux tubes, the waves are transverse and longitudinal tube waves. Because of the density stratification the waves are dispersive and have cutoffs: for the acoustic waves in the nonmagnetic medium and for longitudinal flux tube waves, the period is about three minutes; and for transverse flux tube waves, it is about seven minutes for typical values of the observed strength of the magnetic field.

Wave propagation in the nonmagnetic medium is described in terms of plane and spherical waves and excitation by means of impulsive excitation; and for flux tube waves, by large single impulses and by a fluctuating velocity field. Observational signatures of the various wave types and their effect on chromospheric heating are considered. It is concluded that calcium bright points in the nonmagnetic chromosphere are due to spherical acoustic waves; and that in the magnetic network, transverse waves are more important for the oscillations than longitudinal waves and may penetrate into the corona, giving rise to some coronal heating.

1.1 Introduction

The quiet chromosphere is bifurcated into magnetic and nonmagnetic regions. Although magnetic fields are found everywhere on the Sun they are dynamically unimportant in the interior of supergranulation cells (CI). In the magnetic network on the cell boundary (CB), fields are of decisive importance for the nature of the waves and their propagation characteristics.

In the magnetic network, the field occurs in concentrations of intense magnetic flux that are idealized as tubes in which the contribution of the field to the pressure may exceed that of the gas. A typical photospheric value of the plasma$-\beta$ (the ratio of gas to magnetic pressure, $\beta = 8\pi p/B^2$) is $\beta = 1/3$, for which the gas density in a thin tube is lower than in the ambient medium by a factor of 4.

In the thin-tube approximation, vertical tubes in pressure equilibrium with the outside medium expand upward to conserve magnetic flux. From a low filling factor of 1% in the photosphere the tubes spread to 15% in the layers of formation of the emission features in the H and K lines of ionized calcium (at a height of 1 Mm) and to 100% in the magnetic canopy, often defined as the region above the layer where $\beta = 1$. At some height the idealization of a thin flux tube ceases to be useful.

The nature of the waves that can exist in these two media depends on the magnetic field. In the field-free CI, the restoring forces in the wave equation are pressure and gravity. In the upward direction, only acoustic waves can propagate. The chromospheric oscillations in the CI are therefore due to acoustic waves. In oblique directions, gravity-modified acoustic waves can also contribute (Skartlien, Stein & Nordlund 2000). In flux tubes in the magnetic network, all three restoring forces, namely, pressure, gravity and the magnetic field, can act. But the only important wave types appear to be transverse and longitudinal flux tube waves; the former are mainly magnetic, and the latter, mainly acoustic. Internal gravity waves appear to play no role in any of the chromospheric oscillations. The main effect of gravity is to provide the stratification of the atmosphere which, in turn, is responsible for the dispersion of all waves traveling in the vertical direction, and hence for the existence of cutoffs and limits on the frequency ranges in which the waves can either propagate or are evanescent.

In the cell interior, acoustic waves have a period of three minutes (corresponding to a frequency of ν=5 mHz), and kink waves in the magnetic network have typical periods of seven minutes (ν=2.5 mHz), depending on the strength of the magnetic field; longitudinal flux tube waves also have three-minute period and only a weak dependence on field strength. In all these cases, the waves are propagating if their frequency is higher than the respective cutoff frequency, and evanescent if it is lower.

Chromospheric oscillations are seen most prominently in intensity enhancements of the emission peaks in the cores of the K and H lines of Ca II. In the nonmagnetic cell interior, the bright phase of the oscillations gives rise to K_{2v} and H_{2v} bright points, so called because of the pronounced asymmetry of the line profile which favors the blue emission peaks in the

line cores; these bright regions are also referred to as calcium grains. In the magnetic network, the corresponding features are called network bright points; their line profiles are much less asymmetric.

Oscillations reveal the properties of the medium through which they propagate. But whereas $p-$mode oscillations of the solar interior have low damping and long life time, for some modes corresponding to thousands of wave periods, and therefore reveal the internal solar structure in great detail, chromospheric oscillations are highly damped by shock dissipation and therefore live only for intervals of the order of a few times the wave period before they must be excited again. Chromospheric oscillations tell us mainly about the state of the atmosphere in the layers where the waves arise. An important difference between internal solar and chromospheric oscillations is that the former are resonance oscillations whereas the characteristic frequencies of chromospheric oscillations owe their values to the existence of cutoffs of dispersive waves propagating upward (or downward) in a stratified medium, in which waves with wavelengths much longer than the density scale height propagate with reduced group velocity and, eventually, with the group velocity approaching zero and the phase velocity approaching infinity; in that limit, a wave is evanescent and transports no energy (in the linear limit), and the atmosphere swings in unison, either up and down (acoustic waves) or sideways (transverse flux tube waves).

1.2 Oscillations in the Nonmagnetic Chromosphere

The most important lines for the three-minute oscillations in the nonmagnetic chromosphere have been the H and K lines, with residual central intensity of 4% the strongest lines in the visible solar spectrum. Seminal papers on ground-based observations of oscillations are: Liu (1974); Grossmann-Doerth, v.Uexküll & Kneer (1976); Cram & Damé (1983); v.Uexküll & Kneer (1995); and on space observations by Carlsson, Judge & Wilhelm (1997). The only empirical model of chromospheric oscillations is by Carlsson & Stein (1994, 1997). Important theoretical papers are Lamb(1908), Fleck & Schmitz (1991) and Rossi et al. (1991) for the analytic solution of the wave equation for impulsive excitation of oscillations in a one-dimensional (1D), stratified, isothermal atmosphere; Kalkofen et al. (1994) for the numerical solution in an isothermal atmosphere and Sutmann & Ulmschneider (1995) in an empirical chromospheric model; and Kato (1966) and Bodo et al. (2000) for the analytic solution of the wave equation in three-dimensional geometry.

The wave period was proposed to be due to standing waves in the cav-

ity formed by the chromospheric temperature structure (Leibacher & Stein 1981). That explanation became untenable with the simulation of bright-point oscillations in the dynamical model of Carlsson & Stein (1994). The excitation of oscillations was proposed to be due to internal $p-$modes (e.g. Rutten & Uitenbroek 1991, v.Uexküll & Kneer 1995, Carlsson et al. 1997), which were presumed to generate upward-propagating waves by superposition. Such a model calls for a source region with a linear size of the order of the wavelength of $p-$modes, approximately 2,000 km. But observations of the horizontal size of the propagation channel in which the waves responsible for the oscillations travel upward suggest a size varying between the width of an intergranular lane in the photosphere (Sivaraman, Bagare & November 1990), about 100 km, and about 6,000 km in high layers of the chromosphere (Carlsson et al. 1997). The actual area of the excitation region would thus be smaller by two orders of magnitude than that required for $p-$mode excitation. This mechanism also fails to explain the wave period.

The excitation of bright-point oscillations is still an unsolved problem. The most plausible explanation for the wave period is that it is the acoustic cutoff period in the upper photosphere (discussed below).

Although both calcium bright points and chromospheric heating are caused by acoustic waves, the paucity and location of bright points suggest that they arise in a process that is different from that of the general heating of the chromosphere. For a ratio of $I_{\mathrm{K_{2v}}}/\bar{I} = 1.5$ of the intensity maximum at the $\mathrm{K_{2v}}$ emission peak and the average intensity in the cell interior (in a band of 0.3 Å centered on $\mathrm{K_{2v}}$), v.Uexküll and Kneer found that bright points occur only in 5% to 10% of the CI. Nevertheless, the process of heating the chromosphere is likely to cause some motions of low amplitude with a period of three minutes since the waves generated in the convection zone by the Lighthill mechanism carry a substantial signal at the acoustic cutoff period (Theurer, Ulmschneider & Kalkofen 1997). Thus, a plausible scenario of three-minute oscillations consists of calcium bright points that are caused by discrete excitation processes in intergranular lanes, and of a low-level background of waves with the cutoff period as a signature that are caused by the general heating of the chromosphere.

The oscillations seen in calcium bright points reveal the dynamics and the underlying structure of the chromosphere. An instructive example is the K line observed by Liu (1974) and shown in Figure 1.1 at three phases during the evolution of a wave. At time $t = 0$, the wave is deep in the photosphere and has low amplitude. The intensity profile is symmetric and shows the temperature structure of the undisturbed atmosphere, mapped from depth to wavelength. Following the line intensity inwards from the wings, the

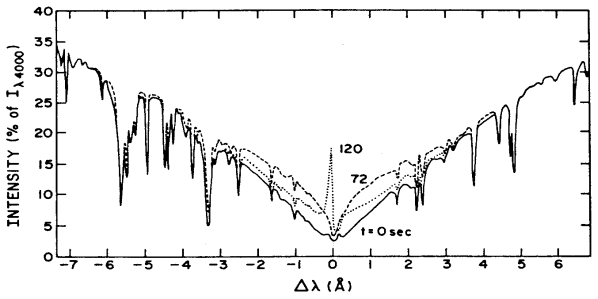

Fig. 1.1. Figure 1. Profile of the K line at three phases in the evolution of an oscillation – from Liu (1974).

temperature drops through the photosphere to symmetrically placed minima in the K line profile, which are formed at the temperature minimum between photosphere and chromosphere. The intensity then rises inward, corresponding to the outward rise of the kinetic temperature, until photons from the line can escape from the atmosphere. At that point the line profile forms the K_2 maxima, where the excitation temperature of the two combining states in the line transition separates from the kinetic temperature and the source function drops below the Planck function; the intensity continues to drop to the line center, forming the K_3 minimum.

At the time of $t = 120$ s, the wave has reached the layer of formation of the K_2 maxima and led to a very large, asymmetrical increase of the intensity of the blue emission peak, K_{2v}. At the same time, the K_3 minimum is shifted towards the red side of the spectrum. The simultaneous intensity enhancement at K_{2v} and the redshift of K_3 is the signature of K_{2v} bright-point oscillations that must be explained by a model of chromospheric dynamics.

The empirical dynamical model by Carlsson & Stein (1994) reproduced these features. Starting from cospatial observations by Lites, Rutten & Kalkofen (1993) of the Doppler velocity of a photospheric Fe I line and of the simultaneous evolution of the H line, Carlsson & Stein drove the lower boundary in their simulation with the observed Doppler velocity. The comparison of the simulated and observed H line intensities as functions of wavelength and time (Figure 1.2: profiles, respectively, on the left and the right) shows broad agreement in the signature feature for the simulated bright point, namely, the simultaneous occurrence of enhancement of the H_{2v} intensity peak and redshift of the line center H_3. These features are formed when the upward-propagating shock wave, which heats the layer where the H_2 emission peaks are formed, meets downward-streaming gas above this

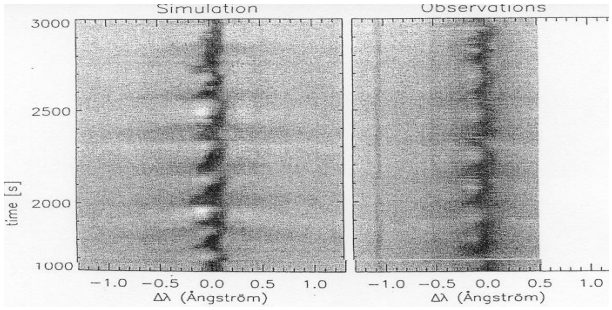

Fig. 1.2. Figure 2. The H line intensity as a function of wavelength and time: left panel, simulated; right panel, observed — from Carlsson (1994).

layer, which had been lifted upwards by the preceding wave. Although this feature has been explained before, from a study of waves in an isothermal atmosphere (Kalkofen et al. 1994), the significance of the Carlsson & Stein simulations is that the intimate relation between waves in the photosphere and subsequent dynamics in the chromosphere was shown in an empirical model. This model established that calcium bright points are caused by propagating acoustic waves and the intermittent formation of shocks. The value of this demonstration is not diminished by the flaws of the model, which are apparent in Fig. 1.2, which is taken from the frontispiece of the Oslo proceedings booklet.

There are three differences between the simulated and the observed intensities. They are the late arrival of the shock in the layer of formation of the blue emission peak, the H_3 intensity formed above the shock that may be low by an order of magnitude, and the H_{2v} intensity at maximal brightness that may be high by an order of magnitude.

The reason for the late arrival of the shock is not understood. The low intensity of the line center was traced to the intermittent heating in the dynamics and the absence of general heating (Kalkofen, Ulmschneider & Avrett 1999, Kalkofen 2001). And the excess intensity at H_{2v} is due to the topology of wave propagation in bright-point oscillations, which the model assumes to be in the form of plane waves, where the energy of the waves is trapped in vertical cylinders, whereas the Sun shows them to be in the form of spherical waves, where the energy spreads horizontally in upward propagation. This spreading is apparent in the size of the area disturbed by the shock and varies from the 100 km in the photosphere, noted above, to 0.5 to 1 Mm at the base of the chromosphere (Foing & Bonnet 1984),

to 2 to 3 Mm in the layer of formation of the H_{2v} emission peak (Cram & Damé 1983).

The main properties of the oscillations can be understood from the linearized hydrodynamic equations. The (1D) equations for plane waves illuminate the role played by the acoustic cutoff frequency, and the 3D solutions show the horizontal spreading of the wave energy.

For the discussion of the equations it is convenient to separate the exponential variation of the physical quantities and to write the equations in terms of their corresponding "reduced" quantities. Thus, instead of the physical velocity $v(z,t)$ in terms of height z and time t we write the hydrodynamic equations for a reduced velocity $u(z,t)$, defined by

$$v(z,t) = u(z,t)\exp(z/2\mathcal{H}). \tag{1.1}$$

The equation expresses the property that the physical velocity grows in the vertical direction with an e-folding distance of twice the density scale height. This vertical growth compensates for the exponential decrease of the density and insures that energy flux is conserved.

The hydrodynamic equations for dimensionless variables z' and t' can be cast into the form of a wave equation, called Klein-Gordon equation,

$$\frac{\partial^2}{\partial z'^2}u - \frac{\partial^2}{\partial t'^2}u - u = 0\ . \tag{1.2}$$

With the ansatz $u(z',t') \sim \exp(ikz' - i\omega t')$, we obtain the dispersion relation for disturbances propagating in this stratified, isothermal medium,

$$k^2 = \omega^2 - 1, \tag{1.3}$$

and the phase and group velocities

$$v_{\rm ph} = \frac{\omega}{k} = \frac{\omega}{\sqrt{\omega^2-1}}, \quad v_{\rm g} = \frac{\partial\omega}{\partial k} = 1/v_{\rm ph}, \quad v_{\rm ph}v_{\rm g} = 1. \tag{1.4}$$

At the cutoff frequency, $\omega = 1$, the phase velocity becomes infinite and the group velocity becomes zero. The product of phase and group velocities equals the square of the sound speed, which is unity here.

The analytic solution of the equations for a velocity pulse (see Kalkofen et al. 1994), which is due to Lamb (1909), shows the pulse propagating with sound speed in the vertical direction, followed by a wake, which in the limit of late times results in a decaying oscillation at the cutoff frequency,

$$u(z',t') \propto \frac{\cos(t')}{\sqrt{t'}}\ . \tag{1.5}$$

It is interesting to note that transverse and longitudinal waves in a thin

flux tube embedded in an isothermal medium obey the same wave equation (1.2); only the transformation (1.1) is modified to allow for the upward expansion of the flux tube to conserve magnetic flux, leading to an e-folding distance for the growth of the velocity amplitude of tube waves of $4\mathcal{H}$.

The three-dimensional hydrodynamic equations describe internal gravity waves in addition to acoustic waves (see Kato 1966). But internal gravity waves are excluded from the vertical direction, and carry little energy in the horizontal direction. Acoustic waves in the horizontal direction suffer only geometrical dilution and are therefore also unimportant for chromospheric oscillations. In the vertical direction, the growth of the "wave amplitude" (for pressure p or v^2) is still proportional to the factor $\exp(z/\mathcal{H})$.

There are two major differences between solutions for acoustic waves in 1D and 3D. In the spherical case, the wave amplitude decreases with the square of the distance from the origin suggesting flux conservation through a spherical surface, and varies along the perimeter of the circle about the source. This is seen in the upper panel of Figure 1.3, where the top curve displays the pulse at the time when its apex has reached the reference height of 15 $\mathcal{H}$ that represents the layer of formation of the H_{2v} and K_{2v} emission peaks, showing the wave amplitude increasing from the pole to the equator (and decreasing again to the south pole). For the oscillations in the wake of the pulse, the energy is reduced — in the third wave, for example, by an order of magnitude — and the amplitude decreases with increasing zenith angle. Thus, the profile of the upward-propagating wave narrows and more energy is concentrated towards the axis of the channel. The lower panel shows the same curves, but with the exponential factor $\exp(z/\mathcal{H})$. The steeper decrease of the amplitudes with angle reflects the lower height reached by parts of the wave at larger angle.

The results from the linear, analytic solution cannot be carried over to the nonlinear regime immediately. In the 1D case, for example, the nonlinear solution no longer has most of the energy in the initial pulse, but in the second or third oscillation in its wake. Similarly, in the numerical simulation of bright-point dynamics by Carlsson & Stein (1994), a calculation for the atmosphere initially at rest shows little correspondence with the observations until a time interval of the order of the wave period.

Among the important results of the 3D calculation is the increase of the phase velocity for the oscillation behind the pulse (only in the vertical direction), the finite width of the propagation channel, and the narrowing of the channel for the later oscillations, with some modification expected for the nonlinear behavior of the waves on the Sun. A prediction from the 3D solution is that a bright point would begin at the center and grow outward.

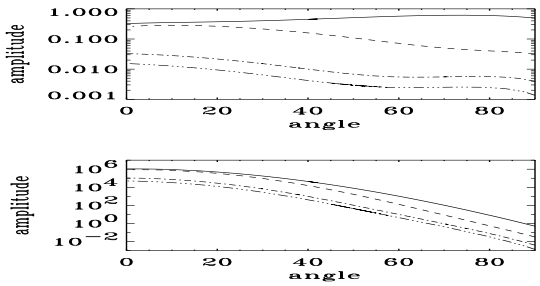

Fig. 1.3. Figure 3. Wave amplitudes in arbitrary units as functions of polar angle in a vertical cut, at the times when the apex of the pulse (top curve) and the apices of the waves in its wake (ordered below the pulse) have reached the target height. Top panel: wave amplitudes without the exponential-growth factor; bottom panel: with the factor — from Bodo et al. (2000).

It would fade the same way and leave behind a bright ring. Another unique feature of calcium bright points in the field-free medium is that the axis of the propagation channel is controlled only by the direction of gravity, and should therefore be vertical, without being inclined as can be the case for waves propagating in magnetic flux tubes.

1.3 Oscillations the Magnetic Network

Ground-based observations of the Ca II H and K lines, which are formed in the low chromosphere, show similar emission from network and internetwork regions. While instantaneous bright points from the internetwork may outshine network bright points (see Fig. 1 of Lites et al. 1993), the long-time average intensity shows total calcium emission from the network to be more important (see Fig. 1 of von Uexküll & Kneer 1995). In addition to the higher intensity of the network bright points, their period is longer, ~ 7 minutes (Lites et al. 1993, Curdt & Heinzel 1998), and the time variation of their intensity profile is much less peaked.

Space-based observations of UV spectral lines and continua provide important constraints on the structure and dynamics of the chromosphere and chromosphere-corona transition region. Observations with SUMER indicate that network regions are brighter than internetwork regions and show strong oscillatory power only at lower frequencies (Judge, Carlsson & Wilhelm 1997). Transition region lines from the network show persistent redshifts and the line widths indicate the presence of subsonic, unresolved nonthermal Doppler motions of several kilometers per second (Dere & Mason 1993;

Peter 2000, 2001). Furthermore, there is a strong correlation between high intensity and redshift (Hansteen, Betta & Carlsson 2000). Curdt & Heinzel (1998) found evidence for upward propagating waves within the network (also see Heinzel & Curdt 1999). However, the wave modes responsible for these oscillations have not yet been identified.

In this section, we shall focus on dynamical processes occuring in the network and their role in heating the magnetic chromosphere. A complete model must explain the nature and period of the oscillations observed in the network as well as its heating. Furthermore, the model must be compatible with observations.

The magnetic field in the network can be idealized in terms of isolated vertical flux tubes in the photosphere which fan out with height. It is well known that flux tubes support a variety of wave modes. The detailed behavior of these modes for thin flux tubes has been extensively studied (for a recent review see Roberts and Ulmschneider 1998). The modes that we shall be concerned with are the sausage or longitudinal mode (Defouw 1976; Roberts & Webb 1978) and the kink or transverse mode (Ryutov & Ryutova 1976; Parker 1979; Spruit 1982).

The earliest studies on MHD wave excitation were based on extensions of the Lighthill (1952) mechanism (Osterbrock 1961; Musielak & Rosner 1987; Collins 1989, 1992). More recently, Musielak et al (1989, 1995), Huang, Musielak & Ulmschneider (1995) and Ulmschneider & Musielak (1998) examined the generation of longitudinal and transverse waves in a flux tube through turbulent motions in the convection zone. An alternative scenario, based on observations of granule motions and G-band bright points in the network by Muller & Roudier (1992) and Muller et al. (1994), suggests that transverse waves can be generated through the impulse imparted by granules to magnetic flux tubes (Choudhuri, Auffret & Priest 1993; Choudhuri, Dikpati & Banerjee 1993; Steiner et al 1998). These investigations suggested that there is sufficient energy flux in MHD waves to account for chromospheric heating.

In this work, we consider in some detail consequences of MHD wave excitation in magnetic flux tubes through the buffeting action of convective motions (granulation) in the surrounding medium. Such waves are likely to play an important role in heating the magnetic chromosphere and also possibly the corona.

Consider a vertical magnetic flux tube extending through the photosphere, which we assume to be "thin" and isothermal. It is convenient again to use the "reduced" displacement, $Q(z,t)$, which for a thin flux tube is related to the physical Lagrangian displacement, $\xi(z,t)$, by $Q(z,t) = \xi(z,t)e^{-z/4\mathcal{H}}$.

It can be shown that Q_α ($\alpha = \kappa$ for transverse waves and $\alpha = \lambda$ for longitudinal waves) satisfies a Klein-Gordon equation (Hasan and Kalkofen 1999, henceforth HK), similar to the case of the non-magnetic medium.

$$\frac{\partial^2 Q_\alpha}{\partial z^2} - \frac{1}{c_\alpha^2}\frac{\partial^2 Q_\alpha}{\partial t^2} - k_\alpha^2 Q_\alpha = F_\alpha, \tag{1.6}$$

where $k_\alpha = \omega_\alpha / c_\alpha$, ω_α is the cutoff frequency for the wave and c_α is the wave propagation speed in the medium and F_α is a forcing function (see HK for details). The speeds for the transverse and longitudinal waves are, respectively,

$$c_\kappa^2 = \frac{2}{\gamma}\,\frac{c_s^2}{1+2\beta},$$

$$c_\lambda^2 = \frac{c_s^2}{1+\gamma\beta/2},$$

where c_s is the sound speed, γ is the ratio of specific heats ($\gamma = 5/3$), $\beta = 8\pi p/B^2$, p is the gas pressure inside the tube and B is the magnitude of the vertical component of the magnetic field on the tube axis.

The cutoff frequencies for transverse and longitudinal waves are, respectively,

$$\omega_\kappa^2 = \frac{g}{8\mathcal{H}}\frac{1}{1+2\beta}, \tag{1.7}$$

$$\omega_\lambda^2 = \omega_{BV}^2 + \frac{c_\lambda^2}{\mathcal{H}^2}\left(\frac{3}{4} - \frac{1}{\gamma}\right)^2, \tag{1.8}$$

where $\omega_{BV}^2 = g^2\,(\gamma - 1)/c_s^2$ is the Brunt-Väisälä frequency.

The solutions of Eq. (1.6) can easily be developed using Green's functions (for details see HK). The generic behavior for the impulsive excitation of transverse and longitudinal waves by granular motions in the magnetic network is the same: the buffeting action due to a single impact excites a pulse that propagates along the flux tube with the kink or longitudinal tube speed. For strong magnetic fields ($\beta < 1$), most of the energy goes into transverse waves, and only a much smaller fraction into longitudinal waves. After the passage of the pulse, the atmosphere gradually relaxes to a state in which it oscillates at the cutoff period of the mode. These results show that the first pulse carries most of the energy and after this pulse has passed the atmosphere oscillates in phase without energy transport. The period observed in the magnetic network is interpreted as the cutoff period

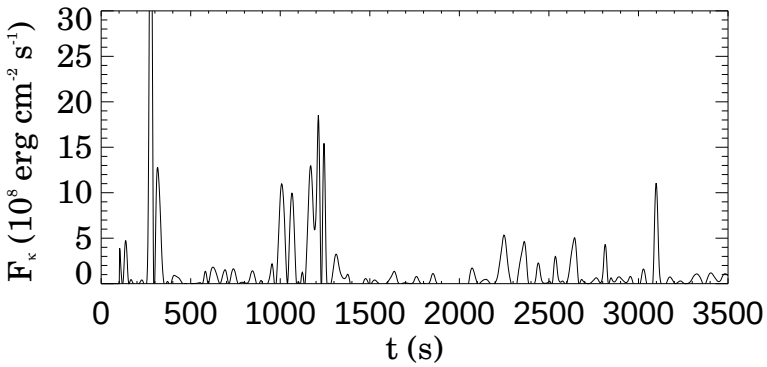

Fig. 1.4. Time variation of the vertical energy flux in transverse waves in a single flux tube at $z = 750$ km due to footpoint motions, taken from observations, excited in an isothermal flux tube with $T = 6650$ K, $\beta = 0.3$.

of transverse waves, which leads naturally to an oscillation at this period (typically in the 7-minute range) as proposed by Kalkofen (1997).

For weaker magnetic fields the energy fluxes in the two modes are comparable. From the absence of a strong peak at low frequencies in the power spectrum of the cell interior (CI) we conclude that both transverse and longitudinal waves must make a negligible contribution to K_{2v} bright point oscillations. The absence of the magnetic modes then implies that the waves in the CI are probably acoustic waves, and the observed 3 minute period is therefore the acoustic cutoff period — and not the cutoff period of longitudinal flux tube waves. This implies that the magnetic field structure in the CI is likely to be different from that of flux tubes in the magnetic network.

The above analysis has considered the buffeting of flux tubes as a single impact. In reality, we expect the excitation of waves in a tube to occur not as a single impact but continually due to the highly turbulent and stochastic motion of granules. It is interesting to examine the consequences of this interaction for chromospheric heating. Such an investigation was carried out by Hasan, Kalkofen & van Ballegooijen (2000, hereafter HKB), who modeled the excitation of waves in the magnetic network due to the observed motions of G-band bright points, which were taken as a proxy for footpoint motions of flux tubes. Using high resolution observations of G band bright points in the magnetic network, the energy flux in transverse waves was calculated in a large number of magnetic elements.

Fig. (1.4) shows the vertical energy flux in transverse waves versus time at a height $z = 750$ km for a typical magnetic element in the network. We find that the injection of energy into the chromosphere takes place in brief

and intermittent bursts, lasting typically 30 s, separated by longer periods (longer than the time scale for radiative losses in the chromosphere) with lower energy flux. The peak energy flux into the chromosphere is as high as 10^9 erg cm^{-2} s^{-1} in a single flux tube, although the time-averaged flux is $\sim 10^8$ erg cm^{-2} s^{-1}. However, from an observational point of view, such a scenario for heating the magnetic network would yield a high variability with time in Ca II emission, which appears incompatible with observations. A possible remedy to this difficulty would be to postulate the existence of other high-frequency motions (periods 5-50 s) which cannot be detected as proper motions of G-band bright points (HKB). Adding such high-frequency motions to the simulations HKB obtained much better agreement with the persistent emission observed from the magnetic network. For a filling factor of 10% at $z = 750$ km, the predicted flux is $\sim 10^7$ erg cm^{-2} s^{-1}, which is sufficient to balance the observed radiative loss of the chromospheric network (see Model F$'$ of Avrett 1985). Therefore, for transverse waves to provide a viable mechanism for *sustained* chromospheric heating, the main contribution to the heating must come from high-frequency motions, with typical periods 5-50 s. HKB speculated that the high-frequency motions could be due to turbulence in intergranular lanes, but whether the level of turbulence is sufficiently high remains to be investigated.

The above studies were based on a linear approximation, in which the longitudinal and transverse waves are decoupled. However, the velocity amplitude $v(z)$ for the two modes increases with height z (for an isothermal atmosphere $v \propto \exp(z/4\mathcal{H})$, where $\mathcal{H}$ is the pressure scale height), so the motions are likely to become supersonic higher up in the atmosphere. At such heights, nonlinear effects become important, leading to coupling between the transverse and longitudinal modes. Some progress on this question has been made using the nonlinear equations for a thin flux tube (Ulmschneider, Zähringer & Musielak 1991; Huang, Ulmschneider & Musielak 1995). This work has been extended to include a treatment of kink and longitudinal shocks (Zhugzhda, Bromm & Ulmschneider 1995).

Recently, Hasan, Kalkofen & Ulmschneider (2001) carried out preliminary adiabatic calculations of nonlinear kink waves in a thin, isothermal flux tube. The footpoints are impulsively shaken with a transverse velocity of the form $v_x(0,t) = v_0 \exp[-(t-t_0)^2/\tau^2]$, where v_0 is the specified velocity amplitude, t_0 is the time of maximum velocity, and τ is the duration of the impulse (the longitudinal velocity at the base is assumed to be zero). This impulse generates a transverse wave that propagates upwards with a phase speed $c_\kappa \approx 7.9$ km s^{-1}. Fig. (1.5a) shows the transverse and longitudinal velocity components as functions of height z at various times. We find that

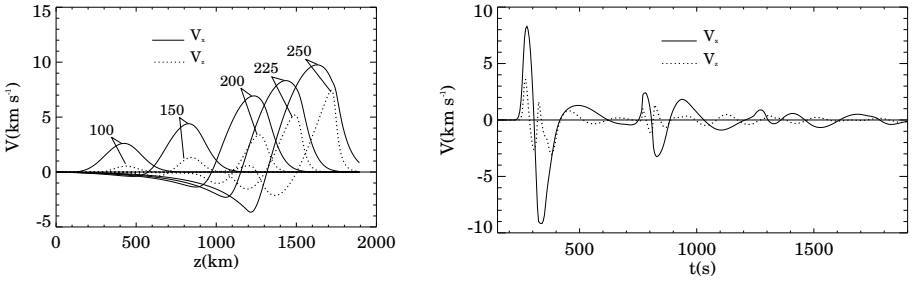

Fig. 1.5. Nonlinear coupling of transverse and longitudinal waves in a flux tube: (**a**) Transverse velocity v_x (*solid curves*) and longitudinal velocity v_z (*dashed curves*) as functions of height z at various times, for $t_0 = 50$ s, $\tau = 20$ s, $v_0 = 1.0$ km s^{-1}. The numbers besides the curves denote time in seconds. (**b**) Velocities as function of time t at a fixed height $z = 1800$ km for $v_0 = 0.75$ km s^{-1}.

in the photospheric layers, where the transverse velocity amplitude is small compared to the kink wave speed, the longitudinal component of the velocity is negligible. However, as the pulse propagates upward the transverse velocity increases and longitudinal motions are generated due to nonlinear effects when $v_x \sim c_\kappa$. The longitudinal motions, being compressive, steepen into shocks. These results are similar to those found by Hollweg, Jackson & Galloway (1982), who studied the nonlinear coupling of torsional Alfvén waves and longitudinal waves. However, in the present calculations we find wakes following the passage of the initial pulse. Fig. (1.5b) shows the velocity as a function of time at a fixed height. Note that at late times the transverse and longitudinal components oscillate with different periods that closely match the cutoff periods (310 s for the kink wave, 230 s for the longitudinal wave). At this stage the velocity amplitudes are small and the two modes are nearly decoupled. This suggests that a power spectrum of network oscillations should detect peaks corresponding to these periods. There is a hint that such peaks may be present in the observations of Lites et al. (1993).

To summarize the main conclusions emerging from the nonlinear calculations: When the transverse velocities are significantly less than the kink wave speed (i.e. the linear regime), there is essentially no excitation of longitudinal waves. However, at heights where $V_x \approx c_\kappa$, longitudinal wave generation becomes efficient, leading to the modes having comparable amplitudes; a large-amplitude transverse pulse generates a longitudinal pulse,

which eventually generates wakes that have low amplitudes and represent decoupled longitudinal and transverse waves, oscillating at their respective cutoff periods. We have examined the coupling between the two modes and find that V_z increases quadratically with V_x at low Mach number M (with respect to c_κ), and linearly with V_x for $M \to 1$. Transverse waves lose energy due to mode coupling. The fractional wave energy in longitudinal motions increases rapidly at first with the forcing transverse velocity V_0, before eventually saturating at a value of about 0.4, which is close to equipartion of energy between the two modes. For a forcing amplitude of $V_0 = 1.5$ km s^{-1}, when there is almost equipartition of energy, the transverse energy flux entering the transition region is approximately 10^7 erg cm^{-2} s^{-1}. This estimate is clearly an upper bound since we need to consider two effects: first, footpoint motions with this velocity occur on average with a frequency of 0.1, and second, there is an attenuation of the flux as it propagates through the transition region, which could lead to a further reduction by a factor of about 10. Hence, we estimate that the net energy flux entering the corona is about 10^5 erg cm^{-2} s^{-1}. Large-amplitude longitudinal waves generated in the upper photosphere steepen and form shocks in the chromosphere. They are likely to be important for chromospheric heating.

References

Avrett E.H. 1985, in: Chromospheric Diagnostics and Modelling, B. Lites Ed., Sunspot NM

Bodo, G., Kalkofen,W., Massaglia, S. & Rossi, P., 2000, A&A 354, 296

Bodo, G., Kalkofen,W., Massaglia, S. & Rossi, P., in: Chromospheric and Coronal Heating Mechanisms, P. Ulmschneider, E. Priest & R. Rosner eds., p353

Carlsson, M. 1994, in Chromospheric Dynamics, Proc. Mini-Workshop, Inst. Theor. Astroph., Oslo, frontispiece

Carlsson, M., Judge, Ph., & Wilhelm, K. 1997, ApJ, 486, L63

Carlsson, M. & Stein, R. F. 1994, in Chromospheric Dynamics, Proc. Mini-Workshop, Inst. Theor. Astroph., Oslo, 47

Carlsson, M. & Stein, R. F. 1997, ApJ 481, 500

Choudhuri, A. R., Auffret, H., & Priest, E. R. 1993, Sol. Phys., 143, 49

Choudhuri, A. R., Dikpati, M., & Banerjee, D. 1993, ApJ, 413, 811

Collins, W. 1989, ApJ, 337, 548

Collins, W. 1992, ApJ, 343, 499

Cram, L. & Damé, L. 1983, ApJ 272, 355

Curdt, W., & Heinzel, P. 1998, ApJ, 503, L95

Defouw, R. J. 1976, ApJ, 209, 266

Dere, K. P., & Mason, H. E. 1993, Sol. Phys., 144, 217

Fleck, B. & Schmitz, F. 1991, A&A 250, 235

Foing, B. & Bonnet, R. M. 1984, ApJ 279, 848

Grossmann-Doerth, U., Kneer, F. & v. Uexküll, M. 1974. Sol. Phys. 37,85

Hansteen, V. H., Betta, R., & Carlsson, M. 2000, A&A, 360, 742

Hasan, S. S., & Kalkofen, W. 1999, ApJ, 519, 899

Hasan, S. S., Kalkofen, W., & van Ballegooijen, A. A. 2000, ApJ, 535, L67

Hasan, S. S., Kalkofen, W., & Ulmschneider, P. 2001, AGU Spring Meeting, abstract SH41B-01

Heinzel, P., & Curdt, W. 1999, in Third Advances in Solar Physics Euroconference: Magnetic Fields and Oscillations, eds. B. Schmieder, A. Hofmann and J. Staude, 201

Hollweg, J. V., Jackson, S., & Galloway, D. 1982, Sol. Phys., 75, 35

Huang, P., Musielak, Z. E., & Ulmschneider, P. 1995, A & A, 297, 579

Judge, P., Carlsson, M., & Wilhelm, K. 1997, ApJ, 490, L195

Kalkofen, W. 1997, ApJ., 486, L148

Kalkofen, W. 2001, ApJ 557, 376

Kalkofen, W., Rossi, P., Bodo, G. & Massaglia, S. 1994, A&A 284, 976
Kalkofen, W. Ulmschneider, P. & Avrett, E. H. 1999, ApJ 521, L141
Kato, S. 1966, ApJ 144, 326
Lamb, H. 1909 Proc. London Math. Soc. (2), 7, 122
Leibacher, J. W. & Stein, R. F. 1981 in: The Sun as a Star, NASA SP-450, 263
Lighthill, M. J. 1952, Proc. Roy. Soc. London, A211, 564
Lites, B. W., Rutten, R. J., & Kalkofen, W. 1993, ApJ, 414, 345
Liu, S.-Y. 1974, Ap. J. 189, 359
Muller, R., & Roudier, Th. 1992, Sol. Phys., 141, 27
Muller, R., Roudier, Th., Vigneau, J., & Auffret, H. 1994, A & A, 283, 232
Musielak, Z. E., & Rosner, R. 1987, ApJ, 315, 371
Musielak, Z. E., Rosner, R., & Ulmschneider, P. 1989, ApJ, 337, 470
Musielak, Z. E., Rosner, R., Gail, H. P., & Ulmschneider, P. 1995, ApJ, 448, 865
Osin, A., Volin, S., & Ulmschneider, P. 1999, A & A, 351, 359
Osterbrock, D. E. 1961, ApJ, 134, 347
Parker, E. N. 1979, Cosmic Magnetic Fields, Clarendon Press, Oxford Peter, H. 2000, A & A, 360, 761
Peter, H. 2001, A & A, 374, 1108
Roberts, B., & Webb, A. R. 1978, Sol. Phys., 56, 5
Roberts, B., & Ulmschneider, P. 1998, in Lecture Notes in Physics, Springer Verlag, Heidelberg, Vol. 489, p. 75
Rutten, R. & Uitenbroek, H. 1991, Solar Phys. 134, 15
Ryutov, D. D., & Ryutova, M. P. 1976, Sov. Phys. J.E.T.P., 43, 491
Sivaraman, K.R., Bagare, S.P. & November, L.J. 1990, in Basis Plasma Processes on the Sun, Dordrecht: Kluwer, 102
Skartlien, R., Stein, R. F. & Nordlund, Å 2000 ApJ 541, 468
Spruit, H. C. 1982, Sol. Phys., 75, 3
Steiner, O., Grossmann-Doerth, U., Knölker, M. & Schüssler, M. 1998, ApJ, 495, 468
Sutmann, G. & Ulmschneider, P. 1995, A&A, 294, 241
Theurer, J., Ulmschneider, P. & Kalkofen, W. 1997 A&A, 324, 717
Ulmschneider, P., & Musielak, Z. E. 1998, A & A, 338, 311
Ulmschneider, P., Zähringer, K., & Musielak, Z. E. 1991, A & A, 241, 625
von Uexküll, M., & Kneer, F. 1995, A&A, 294, 252
Zhugzhda, Y. D., Bromm, V., & Ulmschneider, P. 1995, A & A, 300, 302 579